Inorg. Chem. **2005**, *44*, 2761–2765

Field-Induced Magnetic Transitions in Metal Phosphonates with Ladderlike Chain Structures: $(NH_3C_6H_4NH_3)M_2(hedpH)_2 \cdot H_2O$ [M = Fe, Co, Mn, Zn; hedp = $C(CH_3)(OH)(PO_3)_2$]

Ping Yin,[†] Song Gao,[‡] Zhe-Ming Wang,[‡] Chun-Hua Yan,[‡] Li-Min Zheng,*[,†] and Xin-Quan Xin[†]

State Key Laboratory of Coordination Chemistry, Coordination Chemistry Institute, Nanjing University, Nanjing 210093, People's Republic of China, and State Key Laboratory of Rare Earth Materials and Applications, College of Chemistry and Molecular Engineering, Peking University, Beijing 100871, People's Republic of China

Received November 6, 2004

This paper reports the syntheses and characterization of four isomorphous compounds $(NH_3C_6H_4NH_3)M_2(hedpH)_2 \cdot H_2O$ [M = Fe (**1**), Co (**2**), Mn (**3**), Zn (**4**); hedp = $C(CH_3)(OH)(PO_3)_2$]. Each contains two crystallographically different kinds of $\{M_2(hedpH)_2\}_n$ double chains, where the $\{M_2(\mu\text{-}O)_2\}$ dimer units are connected by O–P–O bridges. The double chains are connected through extensive hydrogen bonds, hence generating a three-dimensional supramolecular network. The temperature-dependent magnetic susceptibility measurements show dominant antiferromagnetic interactions in compounds **1**–**3**, mediated through the μ-O and/or O–P–O bridges between the metal(II) centers. The magnetization measurements reveal that compounds **1**–**3** experience field-induced magnetic transitions at low temperatures.

Introduction

The design and syntheses of paramagnetic molecular solids with ladderlike chain structures are of great importance because of the current interest in quantum antiferromagnetic spin ladders.[1−3] Magnetic spin ladders can be viewed as a class of low-dimensional materials with structural and physical properties between those of 1D chains and 2D planes. In an ideal spin ladder, the exchange coupling along the rungs ($J_\perp$) is very similar to that along the chains ($J_{||}$), but each ladder is well isolated from its equivalent neighbors, i.e., interladder $J' \ll J_{||}, J_\perp$. In the presence of an external magnetic field, spin ladders can experience a transition from a nonmagnetic ground state to a spin-polarized state. When doped with charge carriers, an even-leg ladder is predicted to become a superconductor. Therefore, many efforts are being made to search for new spin ladder systems, mostly with spin $S = 1/2$.[4]

Metal phosphonates are organic−inorganic hybrid materials in which the nature of the organic moiety may be designed to confer specific properties.[5] By using (1-hydroxyethylidene)diphosphonate [hedp, $CH_3C(OH)(PO_3)_2$], we have synthesized a series of M−hedp compounds with double chain structures.[6−10] Some of them contain paramagnetic

* Author to whom correspondence should be addressed. E-mail: lmzheng@netra.nju.edu.cn. Fax: +86-25-83314502.
[†] Nanjing University.
[‡] Peking University.

(1) Sachdev, S. *Science* **2000**, *288*, 475.
(2) Carlin, R. L. *Magnetochemistry*; Springer-Verlag: Berlin, Heidelberg, Germany, 1986.
(3) Rovira, C. *Chem.—Eur. J.* **2000**, *6*, 1723.
(4) For example: (a) Watson, B. C.; Kotov, V. N.; Meisel, M. W.; Hall, D. W.; Granroth, G. E.; Montfrooij, W. T.; Nagler, S. E.; Jensen, D. A.; Backov, R.; Petruska, M. A.; Fanucci, G. E.; Talham, D. R. *Phys. Rev. Lett.* **2001**, *86*, 5168. (b) Willett, R. D.; Galeriu, C.; Landee, C. P.; Turnbull, M. M.; Twamley, B. *Inorg. Chem.* **2004**, *43*, 3804. (c) Oosawa, A.; Katori, H. A.; Tanaka, H. *Phys. Rev. B* **2001**, *63*, 134416. (d) Azuma, M.; Hiroi, Z.; Takano, M.; Ishida, K.; Kitaoka, Y. *Phys. Rev. Lett.* **1994**, *73*, 3463.
(5) For example: (a) Clearfield, A. In *Progress in Inorganic Chemistry*; Karlin, K. D., Ed.; John Wiley & Sons: New York, 1998; Vol. 47, pp 371−510 and references therein. (b) Barthelet, K.; Nogues, M.; Riou, D.; Ferey, G. *Chem. Mater.* **2002**, *14*, 4910. (c) Finn, R. C.; Zubieta, J.; Haushalter, R. C. *Prog. Inorg. Chem.* **2003**, *51*, 421. (d) Stock, N.; Stucky, G. D.; Cheetham, A. K. *Chem. Commun.* **2000**, 2277. (e) Ngo, H. L.; Lin, W. B. *J. Am. Chem. Soc.* **2002**, *124*, 14298.
(6) (a) Zheng, L.-M.; Song, H.-H.; Lin, C.-H.; Wang, S.-L.; Hu, Z.; Yu, Z.; Xin, X.-Q. *Inorg. Chem.* **1999**, *38*, 4618. (b) Song, H.-H.; Zheng, L.-M.; Zhu, G.; Shi, Z.; Feng, S.; Gao, S.; Xin, X.-Q. *Chin. J. Inorg. Chem.* **2002**, *18* (1), 67.
(7) Yin, P.; Gao, S.; Zheng, L.-M.; Xin, X.-Q. *Chem. Mater.* **2003**, *15*, 3233.
(8) Zheng, L.-M.; Gao, S.; Yin, P.; Xin, X.-Q. *Inorg. Chem.* **2004**, *43*, 2151.
(9) Song, H.-H.; Yin, P.; Zheng, L.-M.; Korp, J. D.; Jacobson, A. J.; Xin, X.-Q. *J. Chem. Soc., Dalton Trans.* **2002**, 2752.

10.1021/ic048437l CCC: $30.25
Published on Web 03/24/2005

Table 1. Crystallographic Data for Compounds **1**−**4**

param	**1**	**2**	**3**	**4**
empirical formula	$C_{10}H_{22}Fe_2N_2O_{15}P_4$	$C_{10}H_{22}Co_2N_2O_{15}P_4$	$C_{10}H_{22}Mn_2N_2O_{15}P_4$	$C_{10}H_{22}Zn_2N_2O_{15}P_4$
fw	645.88	652.04	644.06	664.92
cryst system	triclinic	triclinic	triclinic	triclinic
space group	$P\bar{1}$	$P\bar{1}$	$P\bar{1}$	$P\bar{1}$
a, Å	5.5222(11)	5.4651(14)	5.6083(2)	5.48950(10)
b, Å	12.403(3)	12.406(3)	12.4098(4)	12.3661(3)
c, Å	15.454(3)	15.362(4)	15.5105(7)	15.4141(4)
α, deg	87.71(3)	87.452(4)	87.8985(13)	87.5050(10)
β, deg	89.57(3)	88.909(4)	89.9113(13)	89.7740(10)
γ, deg	78.10(3)	78.415(4)	77.536(2)	78.5810(10)
V, Å^3	1034.9(4)	1019.3(5)	1053.33(7)	1024.67(4)
Z	2	2	2	2
D, g·cm^{-3}	2.073	2.125	2.031	2.155
F(000)	656	660	652	672
goodness-of-fit on F^2	0.991	0.984	0.959	0.969
μ(Mo Kα), cm^{-1}	17.93	20.24	15.83	27.36
R_1, wR_2 [$I > 2\sigma(I)$][a]	0.0387, 0.0787	0.0321, 0.0816	0.0438, 0.0757	0.0396, 0.0764
R_1, wR_2(all data)[a]	0.0737, 0.0883	0.0397, 0.0927	0.1073, 0.0898	0.0811, 0.0873
$(\Delta\rho)_{max}$, $(\Delta\rho)_{min}$, e Å^{-3}	0.535, −0.577	0.637, −0.516	0.536, −0.581	0.645, −0.566

[a] $R_1 = \Sigma||F_0| - |F_c||/\Sigma|F_o|$, $wR_2 = [\Sigma w(F_o^2 - F_c^2)/\Sigma w(F_o^2)^2]^{1/2}$.

ladderlike motifs of $\{M_2(hedpH)_2\}_n^{2n-}$ (M = Mn, Fe, Co)[6−9] in which edge-shared MO_6 octahedra are bridged by O−P−O units. Very strong hydrogen bond interactions exist between the chains. These compounds could exhibit quasi-spin ladder behaviors as indicated by the observation of field-induced magnetic transitions at experimentally accessible external fields for compounds $(NH_4)_2M_2(hedpH)_2$ (M = Co, Fe)[7] and $[NH_3(CH_2)_nNH_3]Co_2(hedpH)_2{\cdot}2H_2O$ (n = 4, 5).[8] In compound $[NH_3(CH_2)_5NH_3]Co_2(hedpH)_2{\cdot}2H_2O$, however, a three-dimensional canted antiferromagnetism was observed at very low temperature. To achieve more "isolated" chains of $\{M_2(hedpH)_2\}_n^{2n-}$ and thus to remarkably reduce the interchain couplings, one approach is to insert bigger and more rigid counterions between the anionic double chains. Meanwhile, the introduction of different counterions may also pose influences on the bond lengths and angles within the chain. With the aim at studying the correlation between the crystal structures and the magnetic properties of these chain compounds, we herein report the structures and magnetic properties of four new compounds, namely, $(NH_3C_6H_4NH_3)M_2(hedpH)_2{\cdot}H_2O$ [M = Fe (**1**), Co (**2**), Mn (**3**), Zn (**4**)], where the rigid *p*-phenylenediamine has been employed as template.

Experimental Section

Materials and Methods. All the starting materials were obtained from commercial sources and were used without further purification. The elemental analyses were performed using a PE240C elemental analyzer. The infrared spectra were recorded on a VECTOR 22 FT-IR spectrometer with pressed KBr pellets. The powder XRD patterns were recorded on a Shimadzu XD-3A X-ray diffractometer. Magnetic susceptibility data were obtained on polycrystalline samples of **1**−**3** using an Oxford Maglab magnetometer.

Synthesis of $(NH_3C_6H_4NH_3)M_2(hedpH)_2{\cdot}H_2O$ [M = Fe (1), Co(2), Mn (3), Zn (4)]. The four compounds were synthesized under very similar experimental conditions. In a typical reaction, a mixture of $FeSO_4{\cdot}7H_2O$ (0.2792 g, 1 mmol), 50% $hedpH_4$ (1 cm^3, 2.5 mmol), NaF (0.0425 g, 1 mmol), *p*-phenylenediamine (0.2246 g, 2 mmol), and H_2O (8 cm^3) was heated under stirring. The clear filtrate (pH = 2−3) was transferred directly to a Teflon-lined stainless autoclave (25 cm^3) and heated at 140 °C for 48 h. After slow cooling to room temperature, the light yellow needlelike crystals of compound **1** were collected as a monophasic material, judged by powder XRD measurements. Yield: 56% based on Fe. Anal. Calcd for $C_{10}H_{22}Fe_2N_2O_{15}P_4$: C, 18.58; H, 3.41; N, 4.33. Found: C, 19.62; H, 4.09; N, 4.96. IR (KBr, cm^{-1}): 3394 s, 2855 br, 2067 w, 1939 w, 1628 m, 1563 m, 1526 s, 1423 w, 1339 w, 1181 s, 1098 s, 999 s, 992 s, 797 m, 669 m, 577 m, 433 w.

Data for Compound 2. Yield: 54% based on Co. Anal. Calcd for $C_{10}H_{22}Co_2N_2O_{15}P_4$: C, 18.41; H, 3.37; N, 4.30. Found: C, 18.28; H, 4.03; N, 3.70. IR (KBr, cm^{-1}): 3394 s, 2768 br, 2060 w, 1938 w, 1673 m, 1561 s, 1526 s, 1421 w, 1337 w, 1185 s, 1115 s, 996 s, 921 s, 795 m, 671 m, 578 m, 434 w.

Data for Compound 3. Yield: 55% based on Co. Anal. Calcd for $C_{10}H_{22}Mn_2N_2O_{15}P_4$: C, 18.63; H, 3.42; N, 4.35. Found: C, 19.84; H, 4.65; N, 5.06. IR (KBr, cm^{-1}): 3384 s, 2876 br, 2072 w, 1942 w, 1613 m, 1566 m, 1461 w, 1376 w, 1181 s, 1116 s, 995 s, 924 s, 797 m, 666 m, 575 m, 432 w.

Data for Compound 4. Yield: 53% based on Zn. Anal. Calcd for $C_{10}H_{22}Zn_2N_2O_{15}P_4$: C, 18.07; H, 3.31; N, 4.22. Found: C, 19.04; H, 4.24; N, 4.93. IR (KBr, cm^{-1}): 3411 s, 2764 br, 2061 w, 1936 w, 1626 m, 1561 m, 1525 s, 1422 w, 1335 w, 1179 s, 1113 s, 997 s, 930 s, 797 m, 671 m, 566 m, 411 w.

The sodium fluoride was added to improve the crystallization of the final products. The same compounds were obtained in the absence of NaF.

Crystallographic Studies. Single crystals of dimensions 0.06 × 0.14 × 0.17 mm for **1**, 0.35 × 0.10 × 0.10 mm for **2**, 0.05 × 0.10 × 0.35 mm for **3**, and 0.08 × 0.20 × 0.25 mm for **4** were used for structural determinations. Data collections for compounds **1**, **3**, and **4** were made on a NONIUS KAPPA CCD diffractometer and for compound **2** on a Bruker SMART APEX CCD diffractometer using graphite-monochromatized Mo Kα radiation (λ = 0.710 73 Å) at room temperature. Intensity data were collected in the θ ranges 3.56−27.50° for **1**, 2.10−28.02° for **2**, 3.56−27.98° for **3**, and 3.56−27.5° for **4**. The number of measured and observed reflections [$I > 2\sigma(I)$] are 30 873 and 3259 (R_{int} = 0.0817) for **1**, 6340 and 3646 (R_{int} = 0.0444) for **2**, 20 472 and 2815 (R_{int} = 0.0925) for **3**, and 19 616 and 3080 (R_{int} = 0.0821) for **4**, respectively. Empirical absorption corrections were applied for all

(10) Song, H.-H.; Zheng, L.-M.; Wang, Z.; Yan, C.-H.; Xin, X.-Q. *Inorg. Chem.* **2001**, *40*, 5024.

Table 2. Selected Bond Lengths (Å) and Bond Angles (deg) for Compounds **1**−**4**[a]

	1	2	3	4
M(1)−O(1)	2.050(2)	2.028(2)	2.104(2)	1.998(2)
M(1)−O(2A)	2.073(2)	2.052(2)	2.113(3)	2.001(2)
M(1)−O(5B)	2.110(2)	2.070(2)	2.176(2)	2.055(2)
M(1)−O(4)	2.150(2)	2.124(2)	2.156(2)	2.082(3)
M(1)−O(2B)	2.299(2)	2.249(2)	2.381(2)	2.455(2)
M(1)−O(7B)	2.326(2)	2.267(2)	2.351(3)	2.330(3)
M(2)−O(11)	2.062(2)	2.048(2)	2.096(2)	2.014(2)
M(2)−O(9C)	2.065(2)	2.049(2)	2.110(2)	2.003(2)
M(2)−O(8)	2.106(2)	2.066(2)	2.141(2)	2.048(3)
M(2)−O(12D)	2.151(2)	2.106(2)	2.186(2)	2.099(2)
M(2)−O(14D)	2.218(2)	2.174(2)	2.283(3)	2.186(3)
M(2)−O(9D)	2.300(2)	2.245(2)	2.377(2)	2.429(2)
P(1)−O(1)	1.519(2)	1.510(2)	1.519(2)	1.522(2)
P(1)−O(3)	1.521(2)	1.520(2)	1.527(3)	1.522(3)
P(1)−O(2)	1.534(2)	1.534(2)	1.529(3)	1.526(3)
P(2)−O(4)	1.508(2)	1.512(2)	1.512(2)	1.513(2)
P(2)−O(5)	1.520(2)	1.526(2)	1.515(3)	1.523(3)
P(2)−O(6)	1.539(2)	1.538(2)	1.535(3)	1.530(3)
P(3)−O(8)	1.508(2)	1.510(2)	1.513(2)	1.512(2)
P(3)−O(9)	1.525(2)	1.528(2)	1.524(2)	1.518(3)
P(3)−O(10)	1.531(2)	1.536(2)	1.534(3)	1.535(3)
P(4)−O(11)	1.492(2)	1.493(2)	1.492(2)	1.493(2)
P(4)−O(12)	1.515(2)	1.518(2)	1.515(2)	1.515(3)
P(4)−O(13)	1.570(2)	1.571(2)	1.569(3)	1.567(3)
O(1)−M(1)−O(2A)	99.40(9)	97.93(8)	101.18(10)	100.82(10)
O(1)−M(1)−O(5B)	165.81(9)	167.61(8)	164.61(10)	161.29(11)
O(2A)−M(1)−O(5B)	93.45(9)	93.66(8)	91.81(9)	93.44(10)
O(1)−M(1)−O(4)	89.99(8)	90.75(8)	89.91(9)	93.53(10)
O(2A)−M(1)−O(4)	107.71(9)	104.55(9)	109.26(10)	108.17(11)
O(1)−M(1)−O(2B)	94.91(8)	94.31(8)	94.74(9)	91.14(9)
O(2A)−M(1)−O(2B)	77.99(9)	79.61(8)	77.59(10)	77.41(10)
O(5B)−M(1)−O(2B)	81.84(8)	83.47(8)	79.91(9)	80.12(9)
O(4)−M(1)−O(2B)	171.81(8)	172.96(8)	170.86(9)	171.86(9)
O(1)−M(1)−O(7B)	88.50(9)	88.86(8)	88.58(9)	84.43(10)
O(2A)−M(1)−O(7B)	155.37(8)	158.39(8)	152.37(9)	151.95(10)
O(5B)−M(1)−O(7B)	77.32(8)	78.75(8)	76.14(9)	77.35(9)
O(4)−M(1)−O(7B)	95.49(9)	95.80(8)	96.41(10)	98.88(10)
O(9C)−M(2)−O(8)	99.28(9)	98.05(8)	101.24(10)	100.04(10)
O(11)−M(2)−O(12D)	91.21(9)	90.01(9)	92.67(9)	92.53(10)
O(9C)−M(2)−O(12D)	92.96(9)	93.19(8)	91.32(10)	92.46(10)
O(8)−M(2)−O(12D)	167.14(9)	168.55(8)	166.28(10)	165.05(10)
O(11)−M(2)−O(14D)	101.70(9)	102.57(9)	103.62(10)	105.23(10)
O(11)−M(2)−O(9D)	176.53(8)	154.01(8)	157.13(8)	176.27(10)
O(9C)−M(2)−O(9D)	76.61(9)	89.73(9)	89.90(8)	75.42(10)
O(8)−M(2)−O(9D)	93.50(8)	77.49(9)	78.84(8)	90.62(9)
O(12D)−M(2)−O(9D)	85.46(8)	87.06(8)	83.59(9)	84.58(9)
O(14D)−M(2)−O(9D)	78.56(8)	80.04(7)	76.59(8)	76.52(9)
M(1A)−O(2)−M(1D)	102.01(9)	100.39(8)	102.41(10)	102.59(10)
M(2C)−O(9)−M(2B)	103.39(9)	101.85(8)	103.74(9)	104.58(10)

[a] Symmetry codes: (A) $-x+2, -y+1, -z$; (B) $x+1, y, z$; (C) $-x+1, -y, -z+1$; (D) $x-1, y, z$.

four compounds. The structures were solved by direct methods and refined on F^2 by a full-matrix least-squares procedure using SHELXL 97.[11] All the non-hydrogen atoms were refined anisotropically. Hydrogen atoms were found by Fourier syntheses or included at calculated positions with isotropic thermal parameters proportional to those of the connected atoms. All hydrogen atoms were refined isotropically. Crystallographic and refinement details are listed in Table 1, with selected bond lengths and angles in Table 2 for **1**−**4**.

Results and Discussion

Crystal Structures. Compounds **1**−**4** are isomorphous. All crystallize in space group $P\bar{1}$. Figure 1 depicts a fragment

(11) Sheldrick, G. M. *SHELXTL PC*, version 5; Siemens Analytical X-ray Instruments Inc.: Madison, WI, 1995.

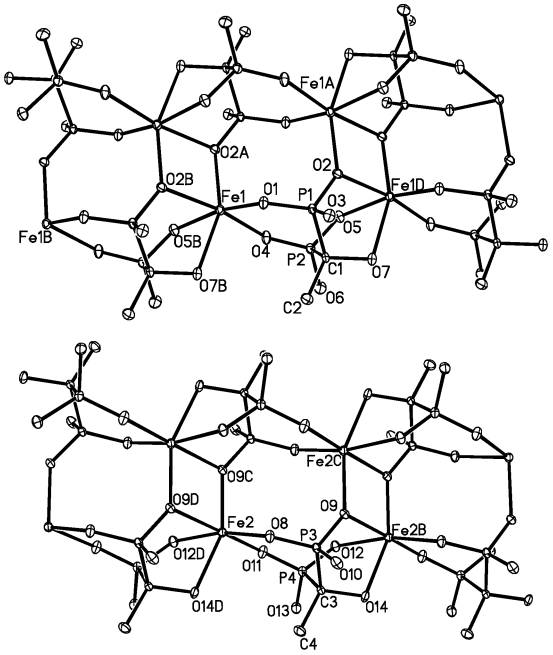

Figure 1. Fragments of chains I (top) and II (bottom) in compound **1**.

of two crystallographically different double chains of compound **1** with the atomic labeling scheme, which contain centrosymmetric dimer units of $Fe_2(hedpH)_2^{2-}$. In double chain I, each Fe atom adopts a distorted octahedral coordination geometry with the six O atoms from three equivalent $hedpH^{3-}$ ligands. The Fe(1)−O bond lengths fall in the range 2.050(2)−2.326(2) Å. These values are close to those in $[NH_3(CH_2)_4NH_3]Fe_2(hedpH)_2\cdot 2H_2O$ [2.066(2)−2.312(2) Å].[6a] The $hedpH^{3-}$ ligand is bis-chelated and bridges the Fe(1) atoms through the O(1), O(2), O(4), and O(5) atoms from phosphonate moieties and O(7) from the hydroxy group. The O(2) atom serves as a μ_3 bridging ligand which links the two iron octahedra through edge sharing, forming infinite double chains along the [100] direction (Figure 1a). The double chain II is very similar (Figure 1b). The Fe···Fe distances over the μ_3-O bridges (along the rung) are 3.401 Å for Fe(1A)···Fe(1D) and 3.429 Å for Fe(2B)···Fe(2C). Those across the O−P−O bridges (along the leg and diagonal) are 5.522 and 4.721 Å for Fe(1)···Fe(1D) and Fe(1)···Fe(1A) and 5.522 and 4.730 Å for Fe(2)···Fe(2B) and Fe(2)···Fe(2C), respectively. The Fe−O−Fe bond angles are 102.01(9)° for Fe(1A)−O(2)−Fe(1D) and 103.39(9)° for Fe(2B)−O(9)−Fe(2C). Between chains I and II, there exist strong hydrogen-bonding interactions. The O(6)···O(10^{i}) and O(13)···O(3) distances are 2.456(3) and 2.532(3) Å, respectively (symmetry code for i: $x, y+1, z$). A three-dimensional supramolecular network structure is therefore constructed by the assembly of two kinds of $\{Fe_2(hedpH)_2\}_n^{2n-}$ chains through strong hydrogen bonding, with one-dimensional channels created along the *a* axis (Figure 2). The $NH_3C_6H_4NH_3^{2+}$ cations are locked inside the channels by three NH···O hydrogen bonds at each end. The bond lengths and angles for $NH_3C_6H_4NH_3^{2+}$ are normal. The lattice water also resides inside the channel forming hydrogen bonds with the phosphonate or the hydroxy oxygen atoms from the chains.

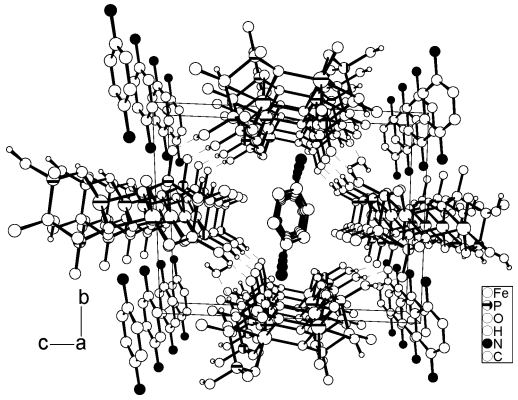

Figure 2. Structure of **1** packed along the *a*-axis.

Table 3. M−O−M Angles (deg) and Critical Fields H_c at 1.8 K (kOe) for Related Compounds with Double Chain Structures

compd	M−O−M angle	H_c	ref
$(NH_4)_2Fe_2(hedpH)_2$	101.6(1)	40	7
$(NH_4)_2Co_2(hedpH)_2$	100.2(1)	35	7
$[NH_3(CH_2)_4NH_3]Co_2(hedpH)_2{\cdot}2H_2O$	98.8(1)	25	8
$[NH_3(CH_2)_5NH_3]Co_2(hedpH)_2{\cdot}2H_2O$	100.5(1)	27.5	8
$(NH_3C_6H_4NH_3)Fe_2(hedpH)_2{\cdot}H_2O$	102.0(1), 103.4(1)	30	this work
$(NH_3C_6H_4NH_3)Co_2(hedpH)_2{\cdot}H_2O$	100.4(1), 101.9(1)	27.5	this work
$(NH_3C_6H_4NH_3)Mn_2(hedpH)_2{\cdot}H_2O$	102.4(1), 103.7(1)	15.5, 32.5	this work

The structures of compounds **2**−**4** are identical with that of **1**, except that the Fe atom in **1** is substituted by Co in **2**, Mn in **3**, or Zn in **4**. Consequently, the M···M distances across the μ_3-O bridges are 3.307 and 3.336 Å for **2**, 3.507 and 3.533 Å for **3**, and 3.489 and 3.516 Å for **4**. The M−O−M bond angles are 100.39(8) and 101.85(8)° for **2**, 102.41(10) and 103.74(9)° for **3**, and 102.59(10) and 104.58(10)° for **4**, respectively. These values are close to those for compound **1**. The XRD measurements reveal that the supramolecular structures of **1**−**4** are maintained after the removal of the lattice water molecules.

The open network structures of **1**−**4** are analogous to those of $[NH_3(CH_2)_nNH_3]M_2(hedpH)_2{\cdot}xH_2O$ (n = 4, 5; M = Fe,[6] Co,[8] Mn,[9] Zn[10]), where flexible alkylenediamines were employed as templates. In the latter cases, however, only one type of double chain is found. Since the protonated alkylenediamines can be contorted to fit into the channels, the very strong interchain hydrogen bond interactions (O···O: ∼2.4 Å) remained in two directions. The employment of rigid *p*-phenylenediamine as template not only results in the formation of two crystallographically distinguished double chains of $\{M_2(hedpH)_2\}_n$ in **1**−**4** but also weakens the interchain hydrogen bond interactions in one direction. Therefore the interchain O···O distances become 2.456(3) and 2.532(3) Å for **1**. In addition, the influence of the cationic counterions on the structures of compounds **1**−**4** is also reflected in the bond lengths and angles within the double chain, some of which are listed in Table 3.

It is noted that a single type of double chain is also observed in compounds $(NH_4)_2M_2(hedpH)_2$ (M = Fe, Co),[7] where a small cation NH_4^+ is involved. In these cases, however, the chains are packed in quite different way; that is, each double chain is surrounded by 6 equiv instead of 4 equiv as observed in **1**−**4**.

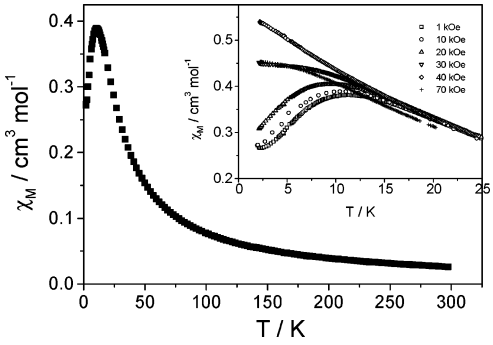

Figure 3. χ_M-T plots for compound **1** at 10 kOe and other external fields (inset).

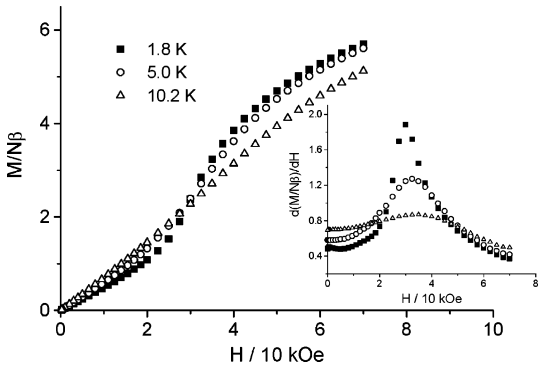

Figure 4. Magnetization of **1** at different temperatures.

Magnetic Properties. Figure 3 shows the temperature-dependent molar magnetic susceptibilities of compound **1** in a magnetic field of 10 kOe. The effective magnetic moment at 300K is 7.91μ_B/molecule, higher than the expected spin-only value for two high-spin Fe(II) centers (μ_{eff} = 6.93 μ_B for g = 2.0), attributed to the orbital contribution. The appearance of a round peak at ca. 11 K in the χ_M versus T curve is typical for a low-dimensional antiferromagnetic system. When the external field is increased, the peak becomes broader and disappears above 30 kOe (Figure 3, inset). The field-dependent magnetization at 1.8 K has a typical S-shaped curve, suggesting a change of the electronic ground state. The critical field, determined by the dM/dH curve, is ca. 30 kOe at 1.8 K (Figure 4). The magnetization at 70 kOe (5.70 $N\beta$) is smaller than the saturation value of 8 $N\beta$ for a pair of S = 2 spins with g = 2.0.

For compounds **2** and **3**, similar magnetic behaviors are observed (Figures 5−8). At 10 kOe, peaks appear in the χ_M vs T curves at ca. 7 and 4 K for **2** and **3**, respectively. Field-induced magnetic transitions due to a change of the electronic ground state are again found. For **2**, the critical field is 27.5 kOe at 1.8 K (Figure 6). The magnetization at 70 kOe is 5.4 $N\beta$/Co_2 unit, higher than the saturation value of 4.6 $N\beta$ anticipated for a pair of S = 1/2 spins with g = 4.6.[12] For **3**, there are two round peaks appearing in the dM/dH vs H curve at 1.8 K, with the transition values of 15.5 and 32.5 kOe, respectively. The magnetization at 70 kOe (10.5 $N\beta$) is close to the saturation value of 10 $N\beta$ for Mn_2 (S = 5/2, g = 2.0).

(12) Caneschi, A.; Dei, A.; Gatteschi, D.; Tangoulis, V. *Inorg. Chem.* **2002**, *41*, 3508.

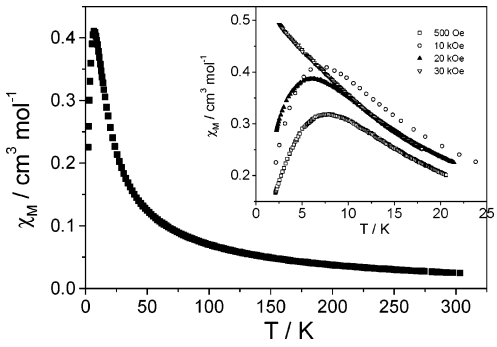

Figure 5. χ_M-T plots for compound **2** at 10 kOe and other external fields (inset).

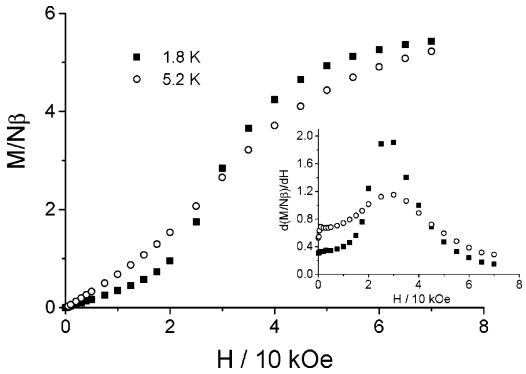

Figure 6. Magnetization of **2** at different temperatures.

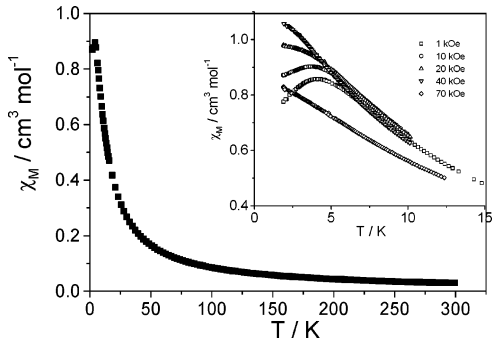

Figure 7. χ_M-T plots for compound **3** at 10 kOe and other external fields (inset).

The observation of field-induced magnetic transitions in compounds **1**−**3** is related to the double chain nature of $\{M_2(hedpH)_2\}_n$. The dominant antiferromagnetic interaction could be propagated within the ladderlike chain through μ-O and/or O−P−O bridges. As the M···M distance over the μ_3-O bridge (3.3−3.5 Å) is much shorter than those over the O−P−O bridges along the leg (5.4−5.6 Å) and the diagonal (4.6−4.8 Å), the exchange coupling through the μ_3-O bridge ($J_\perp$) should be dominant. When the external magnetic field is increased from 0 to 70 kOe, magnetic transitions arising from a change of the electronic ground state occur in **1**−**3**. This phenomenon is similar to those for spin ladder systems. The critical fields, which reflect the spin gap between the singlet ground state and the first excited state, may be related

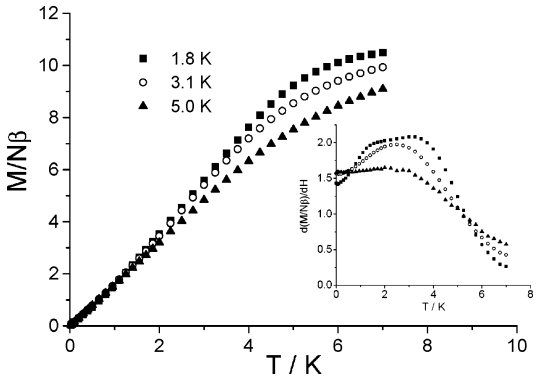

Figure 8. Magnetization of **3** at different temperatures.

to the M−O−M bond angles. Table 3 gives the M−O−M angles and the critical fields obtained for some compounds reported in this work and previous papers. Although no clear clue can be followed, a trend may be found for compounds $[NH_3(CH_2)_nNH_3]Co_2(hedpH)_2\cdot 2H_2O$ (n = 4, 5) and **2** with similar open-network structures. That is, with the Co−O−Co bond angle increasing, the critical field (H_c) becomes larger. It is interesting that, for compound **3**, there appears two critical fields, indicating that a fully polarized state is achieved for this compound below 70 kOe at 1.8 K. Additionally, although low-dimensional antiferromagnetic behaviors are clearly observed for compounds **1**−**3** down to 1.8 K, long-range magnetic ordering below 1.8 K cannot be entirely excluded. Further work is in progress to fully understand the magnetic properties of these systems with ladderlike chain structures.

Conclusion. This paper reports four new isomorphous metal phosphonate compounds based on (1-hydroxyethylidene)diphosphonate: $(NH_3C_6H_4NH_3)M_2(hedpH)_2\cdot H_2O$ (M = Fe, Co, Mn, Zn). Structural analyses reveal that all contain two crystallographically different double chains of $\{M_2(hedpH)_2\}_n$ and the interchain hydrogen bond interactions are weakened in one direction. Field-induced magnetic transitions arising from a change of the electronic ground state are observed for compounds **1**−**3**.

Acknowledgment. Support from the National Natural Science Foundation of China, the Ministry of Education of China, and the Natural Science Foundation of Jiangsu Province (Grant No. BK2002078) is gratefully acknowledged.

Supporting Information Available: Crystallographic data in CIF format. This material is available free of charge via the Internet at http://pubs.acs.org.

IC048437L